



Nonlinear Guyer–Krumhansl equation and its boundary conditions in nanolayers

Michele Sciacca and David Jou

Abstract. This paper deals with nonlinear effects in the Guyer–Krumhansl equation for nonlocal heat transport, both from the perspective of the boundary conditions (phonon–wall collisions) and of the bulk equation (phonon–phonon collisions) and explores their consequences on the effective thermal conductivity of nanosystems between two parallel layers or in two-dimensional ribbons. The nonlinearity arises from a dependence of the respective mean free paths on the values of the heat flux. The boundary conditions refer to slip heat flow along the limiting walls of the system, analogous to velocity slip flow along the walls in rarefied fluid dynamics. The effective thermal conductivity turns out to depend on the Knudsen numbers related to both mean free paths and on the temperature gradient.

Mathematics Subject Classification. 80A20: Heat and mass transfer, heat flow, 93A30: Mathematical modeling.

Keywords. Phonon hydrodynamics, Heat transport, Guyer–Krumhansl equation.

1. Introduction

The interest in miniaturized systems has fostered new studies in heat transport [1–11] which have led, among other generalizations, to Guyer–Krumhansl equation [12–14] incorporating nonlocal terms related to the relevance of the mean free path of the heat carriers as compared to the size of the system and which provide a mathematical basis to the so-called phonon hydrodynamics [13, 15–22]. Most of the analyses have been mainly focused on the linear approach of the Guyer–Krumhansl partial differential equation, which has led to interesting results allowing for the description of a number of experimental observations, in particular in graphene [23–26] and in silicon nanolayers or boron nitride nanolayers [27–29]. In these systems, it was found that hydrodynamics of phonons is more relevant in two dimensions than in three dimensions for a wider range of temperature.

In this paper, we consider the contribution of the nonlinearity from two different sources, phonon–phonon collisions and phonon–wall collisions, respectively, influencing the bulk Guyer–Krumhansl equation and the boundary conditions. In principle, bigger values of the average heat flux will imply a bigger degree of orientation of the phonons motion in the system, and this will modify the relative contribution of elastic and diffusive collisions against the walls, as well as the contribution of three-phonon collisions in the bulk. Here, we study the cases in which the mean free paths depend on q_1 linearly [i.e., $\ell = \ell_0 + \ell_1 q$] or quadratically [i.e., $\ell = \ell_0 + \ell_2 q^2$]. Another possibility that we have previously examined is that the mean free path may depend on the gradient of the heat flux $\gamma = (\nabla \mathbf{q} : \nabla \mathbf{q})^{1/2}$ in a power-law form [30], analogous to the power-law model of non-Newtonian fluids [31].

In particular, as concrete illustration, we consider a rectangular nanolayer of thickness $2R$ (with R small, of the order of 500–5 nm, for instance), and length L ($L \gg R$) and width D ($D \gg R$) much wider than the thickness and that the mean free path. For the sake of simplicity, we assume that heat flows along the x axis and that it depends only on the transversal position y over the thickness of the layer. In Sect. 2, we present the mathematical model which we present in this paper; in Sect. 3, we

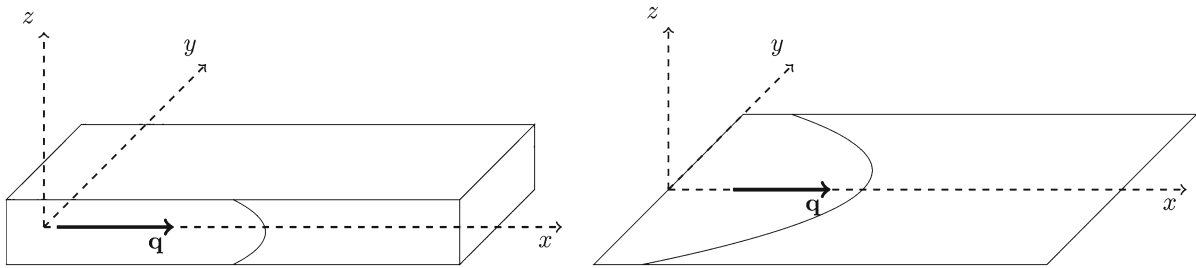


FIG. 1. Heat transport in thin layers (left) and in narrow ribbons (right); \mathbf{q} stands for the local heat flux

consider the linear Guyer–Krumhansl equation with nonlinear boundary conditions; in Sect. 4, the source of nonlinearity is also in the bulk Guyer–Krumhansl equation.

2. Mathematical model

We consider the balance equation for the internal energy u and the Guyer–Krumhansl equation (GK) for the heat flux \mathbf{q} , which are respectively given by [12]

$$\frac{\partial u}{\partial t} + \nabla \cdot \mathbf{q} = 0, \tag{2.1a}$$

$$\tau \frac{\partial \mathbf{q}}{\partial t} + \mathbf{q} = -\lambda \nabla \theta + \ell_b^2 (\nabla^2 \mathbf{q} + \nabla \nabla \cdot \mathbf{q}), \tag{2.1b}$$

where θ designates the temperature [7, 32–34], τ is the relaxation time of the heat carriers, λ is the thermal conductivity, ℓ_b is the mean free path of phonons (related to phonon–phonon collisions), and the subscript “b” stands for bulk. We complement these equations with the boundary condition [5, 15]

$$q_w = -C \ell_w \left(\frac{dq}{d\xi} \right)_{wall}, \tag{2.2}$$

where ℓ_w is the mean free path of the phonons with respect to phonon–wall collisions, q_w is the slip heat flow along the wall, ξ is the outward-pointing variable (in our case y at the wall R and $-y$ at the wall $-R$), and C a numerical constant related to the relative role of specular and diffusive collisions of phonons against the wall. In the usual literature, ℓ_w in (2.2) is assumed to be equal to ℓ_b in (2.1b) and independent of q . In particular, it is derived that for small Knudsen numbers, with $K_n = \ell_0/R$, and with $\ell_0 = \ell_b = \ell_w$, when the term in \mathbf{q} in (2.1b) is negligible with respect to $\ell_b^2 \nabla^2 \mathbf{q}$ in (2.1b), the effective thermal conductivity is [5, 15]

$$K_{eff} = \frac{\lambda}{3K_n^2} + \frac{\lambda C}{2K_n}. \tag{2.3}$$

with the second term taking into account the contribution of the walls.

In this paper, we go beyond this assumption, and we assume that ℓ_b and ℓ_w could be different from each other. Furthermore, ℓ_b and ℓ_w could depend on the applied heat flux, since higher values of \mathbf{q} mean that the motion of heat carriers will be increasingly oriented in the direction of \mathbf{q} and transversal collisions will be less abundant.

Let us assume that $\ell_w(q_n)$, with $q_n = \mathbf{q} \cdot \mathbf{n}$ and \mathbf{n} the wall-normal vector, is a regular function with respect to q_n . Thus, we can consider the expansion into power series of q_n around $q_n = 0$, namely:

$$\ell_w(q_n) = \sum_{i=0}^m \frac{1}{i!} \left[\frac{\partial^i}{\partial q_n^i} \ell_w(q_n) \right]_{q_n=0} q_n^i = \ell_{0w} + \ell_{1w} q_n + \ell_{2w} q_n^2 + \ell_{3w} q_n^3 + \dots \tag{2.4}$$

with ℓ_{iw} the coefficients of the series, namely $\ell_{iw} = \frac{1}{i!} \left[\frac{\partial^i \ell_w(q_n)}{\partial q_n^i} \right]_{q_n=0}$. In the next sections, we use this expansion in the boundary condition (2.2), and we evaluate it for q on the wall.

Let us assume that the bulk mean free path ℓ_b may depend on q_0 , the average value of \mathbf{q} across the layer, namely $q_0 = -K_{eff} \frac{\Delta\theta}{L}$, with K_{eff} the effective thermal conductivity. In particular, we assume that

$$\ell_b(q_0) = \ell_{0b} + \ell'_{0b}(q_0) \quad (2.5)$$

with ℓ_{0b} the usual bulk mean free path of the GK equation, and $\ell'_{0b}(q_0)$ a perturbation of the ℓ_{0b} , which depends on q_0 and it is zero for $q_0 = 0$. Again, we may assume that $\ell'_{0b}(q_0)$ is a regular function of q_0 ; in such a way, we can consider the following expansion in power series around $q_0 = 0$:

$$\ell'_{0b}(q_0) = \sum_{i=0}^m \frac{1}{i!} \left[\frac{\partial^i \ell'_{0b}(q_0)}{\partial q_0^i} \right]_{q_0=0} q_0^i = \ell'_0 + \ell'_1 q_0 + \ell'_2 q_0^2 + \ell'_3 q_0^3 + \dots \quad (2.6)$$

with ℓ'_i the coefficients of the series, namely $\ell'_i = \frac{1}{i!} \left[\frac{\partial^i \ell'_{0b}(q_0)}{\partial q_0^i} \right]_{q_0=0}$. Clearly, the coefficient ℓ'_0 in (2.6) is zero because the perturbation ℓ'_{0b} is zero for $q_0 = 0$. Thus, expression (2.5) becomes

$$\ell_b(q_0) = \ell_{0b} + \ell'_1 q_0 + \ell'_2 q_0^2 + \ell'_3 q_0^3 + \dots \quad (2.7)$$

In this paper, we are interested to consider just the first two terms of the expansion (2.7), as shown in section 4.

Thus, it is interesting to consider both the case in which ℓ_w , ℓ_b or both depends on the heat flux. This is expected to lead to new contributions to K_{eff} , related to the temperature gradient $\Delta\theta$ along the system and to K_n , which we want to evaluate.

3. Nonlinear boundary conditions

In this section, we analyze the contribution of a nonlinear interaction between the heat carriers and the walls. For this reason, we assume that the mean free path ℓ_b in equation (3.8) is constant, but that ℓ_w depends on \mathbf{q} in the boundary condition (2.2) according to (2.4).

Let us consider the nanolayer and narrow ribbon shown in Figure 1 in such a way that the heat flux is along the x -axis and depends on the transversal variable y , and it is independent of the z -axis, namely $\mathbf{q} = q(y)\hat{\mathbf{x}}$. We also assume that the temperature $\theta(x)$ is linear with respect to x , in such a way that the integration of $\nabla\theta$ in $x \in [0, L]$ (L being the length of the nanolayer along x) is $-(\Delta\theta)/L$, with $\Delta\theta$ the difference between the values of θ and at the respective ends of the channel (Fig. 2).

The stationary situation applied to the nanolayer leads to $\nabla \cdot \mathbf{q} = 0$, which is fully satisfied, and to

$$\lambda \frac{\Delta\theta}{L} + \ell_b^2 \frac{d^2 q}{dy^2} = 0, \quad (3.8)$$

where $\partial\mathbf{q}/\partial t = 0$ because of the steady-state condition, and the term in \mathbf{q} on the left-hand side has been neglected because we assume that $\ell^2 \nabla^2 q \gg q$. The latter condition characterizes the so-called hydrodynamic heat transport regime [13, 15–17], as also seen in (2.3).

Substituting the expansion (2.4) in the boundary condition (2.2), we find

$$q_w = -C \ell_w(q) \left(\frac{dq}{d\xi} \right)_{wall} = -C [\ell_{0w} + \ell_{1w} q_w + \ell_{2w} q_w^2 + \ell_{3w} q_w^3 + \dots] \left(\frac{dq}{d\xi} \right)_{wall}. \quad (3.9)$$

For a full analysis of the contribution of the walls, we should take into account the whole expansion of $\ell_w(q)$, but, for the sake of simplicity, we consider the linear case (namely the expansion up to $n = 1$) and a even truncated expansion (for instance, $n = 2$ and the odd coefficient ℓ_{1w} zero).

In the case of a linear dependence of ℓ_w on q , the boundary condition (2.2) becomes

$$q_w = -C (\ell_{0w} + \ell_{1w}q_w) \left(\frac{dq}{d\xi} \right)_{wall} \tag{3.10}$$

where ℓ_{0w} and ℓ_{1w} are two temperature-dependent coefficients, and ℓ_{0w} being the usual phonon mean free path with respect to phonon-wall collisions without the influence of q . In the second case, namely for the even truncated expansion of ℓ_w up to $n = 2$, (3.9) is

$$q_w = -C (\ell_{0w} + \ell_{2w}q_w^2) \left(\frac{dq}{d\xi} \right)_{wall} . \tag{3.11}$$

Assuming that $\ell_{1w} > 0$ (or that $\ell_{2w} > 0$) means that the mean free path increases with the heat flux, i.e., higher \mathbf{q} corresponds to less collisions with the walls because the transversal motion of the phonons is reduced.

In the next two subsections, we consider the mathematical model with the boundary conditions (3.10) (in subsection 3.1) and (3.11) (in subsection 3.2), respectively.

3.1. Nonlinear response on the wall: linear q -dependence of $\ell_w(q)$

The boundary condition (3.10) associated with equation (3.8) may be written as

$$q_w = - \frac{\ell_{0w}C \left(\frac{dq}{d\xi} \right)_{wall}}{1 + \ell_{1w}C \left(\frac{dq}{d\xi} \right)_{wall}} . \tag{3.12}$$

Note that the mathematical consequence of $\ell_{1w} > 0$ in (3.12) is leading to a saturation of the value of the slip heat flow q_w for high values of (dq/dy) at the wall, in contrast to the usual situation corresponding to $\ell_{1w} = 0$. Since dq/dy is of the order of q'_0/R , with q_0 the value of q at the center of the channel, the physical consequences of (3.12) will be relevant for high q'_0 and for small R , namely for thin layers or narrow ribbons and nanowires.

The solution of (3.8) is

$$q(y) = -\lambda \frac{\Delta\theta}{2\ell_b^2 L} y^2 + C_1 + yC_2 \tag{3.13}$$

with C_1 and C_2 numerical constants, and $\ell_b = \ell_{0b}$ because independent of q .

The symmetry request of $q(y)$ with respect to $y = 0$ (the central plane of the layer) leads to $C_2 = 0$. Substituting the solution (3.13) into the boundary condition (3.12), together with the first derivative $\frac{dq}{dy}$ of (3.13) evaluated on the wall, we find the constant C_1 , which is introduced into (3.13).

In this way, the final stationary solution of (3.8) satisfying the boundary condition (3.12) is

$$q(y) = \frac{1}{2} \lambda \frac{\Delta\theta}{L} \left(\frac{R^2}{\ell_b^2} - \frac{y^2}{\ell_b^2} + \frac{2CR\ell_{0w}}{\ell_b^2 - CR\ell_{1w}\lambda\frac{\Delta\theta}{L}} \right) \tag{3.14}$$

which can be written

$$q(y) = \frac{1}{2} \lambda \frac{\Delta\theta}{L} \left(\frac{1}{K_{nb}^2} - \frac{y^2}{\ell_b^2} + \frac{2CK_n}{K_{nb}^2 - CK_{n1}\lambda\frac{\Delta\theta}{L}} \right), \tag{3.15}$$

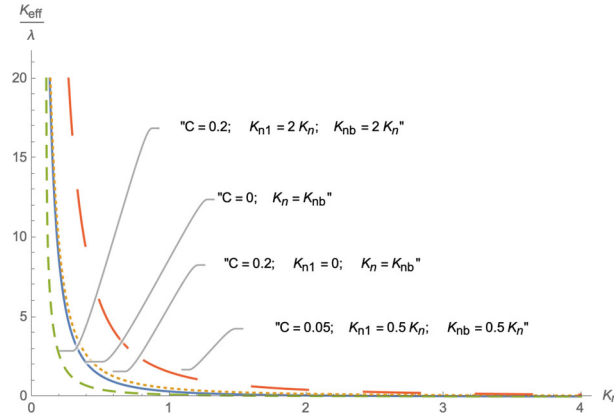


FIG. 2. Plots of K_{eff} (3.17) in terms of the phonon Knudsen number $K_n = \ell_{0w}/R$ for a) $C = 0.2$, $K_{n1} = 2K_n$ and $K_{nb} = 2K_n$; b) $C = 0$ and $K_{nb} = K_n$; c) $C = 0.2$, $K_{n1} = 0$ and $K_{nb} = K_n$; c) $C = 0.05$, $K_{n1} = 0.5K_n$ and $K_{nb} = 0.5K_n$ for a given value $\Delta\theta/L = 1$

where $K_n = \frac{\ell_{0w}}{R}$ is the Knudsen number with reference to the thickness of the layer compared to the wall-mean free path, instead $K_{nb} = \frac{\ell_b}{R}$ is the Knudsen number referred to bulk mean free path, and $K_{n1} = \frac{\ell_{1w}}{R}$.

The heat flux (3.15) consists of two contributions: a) a Poiseuille-like contribution, $\frac{1}{2}\lambda \frac{\Delta\theta}{L} \left(\frac{1}{K_{nb}^2} - \frac{y^2}{\ell_b^2} \right)$, and b) a slip contribution given by $\lambda \frac{\Delta\theta}{L} \frac{CK_n}{K_{nb}^2 - CK_{n1}\lambda \frac{\Delta\theta}{L}}$. Indeed, for $C = 0$ and $\ell_{0w} = \ell_b$, (3.15) yields the typical parabolic profile for Poiseuille phonon flow with nonslip boundary conditions, whereas the term in C gives the influence of the slip flow q_w and the contribution in ℓ_{1w} describes the nonlinear effect.

The effective thermal conductivity of the system is usually defined by

$$K_{eff} = \frac{\int_{-R}^R q(y) dy}{2R} \frac{L}{\Delta\theta}. \quad (3.16)$$

In our case, it will be

$$K_{eff} = \frac{\int_0^R q(y) dy}{R} \frac{L}{\Delta\theta} = \frac{\lambda R^2}{3\ell_b^2} + \frac{C\lambda R\ell_{0w}}{\ell_b^2 - C\lambda\ell_{1w}R\frac{\Delta\theta}{L}} = \frac{\lambda}{3K_{nb}^2} + \frac{C\lambda K_n}{K_{nb}^2 - C\lambda K_{n1}\frac{\Delta\theta}{L}} \quad (3.17)$$

For $C = 0$, K_{eff} would tend to zero as $(R/\ell_b)^2$, for R small. The term in ℓ_{1w} or in K_{n1} makes that K_{eff} depends on $\Delta\theta/L$. Note that for a given value of C but for higher K_{n1} , the effective conductivity becomes smaller as shown in Fig. 2, which is consistent with the fact that, according to (3.12), the higher the ℓ_1 , the smaller the slip heat flow because fast phonons becomes increasingly localized near the central region.

For relatively small values of $K_{n1}(\Delta\theta)/L$, expression (3.17) may be expanded

$$K_{eff} \approx \frac{\lambda}{3K_{nb}^2} + \frac{C\lambda K_n}{K_{nb}^2} \left[1 + C\lambda \frac{\Delta\theta}{L} \frac{K_{n1}}{K_{nb}^2} + \dots \right] \quad (3.18)$$

where we have used the geometric series of reason $a = K_{n1} (\Delta\theta) / L$, namely $\frac{1}{1-a} = 1 + a + a^2 + \dots$

Note that for $(\Delta\theta) / L$ or for K_{n1} sufficiently big, such that the denominator of the second term in (3.17) is very small, this could lead to a negative value for K_{eff} . This would not have a physical meaning because it would violate the second law.

3.2. Nonlinear response on the wall: quadratic q -dependence of $\ell_w(q)$

Here, we still assume that the bulk equation for the heat flux at the steady state is (3.8), and therefore, its solution is (3.13). Instead, we assume that the boundary condition is (3.11) rather than (3.10).

Expression (3.11) leads to

$$q_w = \frac{1}{2C\ell_{2w} \left(\frac{dq}{d\xi}\right)_{wall}} \left(-1 \pm \sqrt{1 - 4C^2\ell_{0w}\ell_{2w} \left(\frac{dq}{d\xi}\right)_{wall}^2} \right), \tag{3.19}$$

which to have a real solution for q_w requires the following condition on the gradient of q at the wall

$$\left(\frac{dq}{dy}\right)_{wall}^2 \leq \frac{1}{4C^2\ell_{0w}\ell_{2w}}. \tag{3.20}$$

This implies that the model (3.11) is more restrictive than model (3.10) with respect to its use in thin layers, because (3.10) may be used for very small R , whereas (3.20) restricts the applicability of (3.11) to situations in which dq/dy , of the order of q'_0/R , is smaller than some specific value. Anyway, we consider also (3.11) in order that our analysis is more complete.

The stationary solution of (3.8) satisfying the boundary condition (3.19) with +sign leads to

$$q(y) = \frac{1}{2} \frac{\lambda}{\ell_b^2} \frac{\Delta\theta}{L} (R^2 - y^2) + \frac{\ell_b^2}{2CR\lambda\ell_{2w} \frac{\Delta\theta}{L}} \left(-1 + \sqrt{1 - \frac{4\lambda^2 \left(\frac{\Delta\theta}{L}\right)^2 C^2\ell_{0w}\ell_{2w}R^2}{\ell_{0b}^4}} \right) \tag{3.21}$$

which is still a Poiseuille-like solution (the first term) plus a slip flow (the second term), as in (3.13).

The effective thermal conductivity as defined by (3.16) is then:

$$\begin{aligned} K_{eff} &= \frac{\lambda}{3} \frac{R^2}{\ell_b^2} + \frac{\ell_b^2}{2CR\lambda\ell_{2w} \left(\frac{\Delta\theta}{L}\right)^2} \left(1 - \sqrt{1 - 4\lambda^2 \left(\frac{\Delta\theta}{L}\right)^2 C^2 R^2 \frac{\ell_{0w}\ell_{2w}}{\ell_{0b}^4}} \right) = \\ &= \frac{\lambda}{3K_{nb}^2} + \frac{K_{nb}^2}{2C\lambda K_{n2} \left(\frac{\Delta\theta}{L}\right)^2} \left(1 - \sqrt{1 - 4\lambda^2 \left(\frac{\Delta\theta}{L}\right)^2 C^2 \frac{K_n K_{n2}}{K_{nb}^4}} \right) \end{aligned} \tag{3.22}$$

where $K_{n2} = \frac{\ell_{2w}}{R}$.

By expanding the root square in (3.22) according to the Taylor series $\sqrt{1-x^2} \approx 1 - x^2/2 - x^4/8$ where $x = 2\lambda \left(\frac{\Delta\theta}{L}\right) C \frac{\sqrt{K_n K_{n2}}}{K_{nb}^2}$, one finds

$$K_{eff} = \frac{\lambda}{3K_{nb}^2} + \lambda C \frac{K_n}{K_{nb}^2} \left(1 + C^2 \lambda^2 \left(\frac{\Delta\theta}{L}\right)^2 \frac{K_n}{K_{nb}^2} \frac{K_{n2}}{K_{nb}^2} \right) \tag{3.23}$$

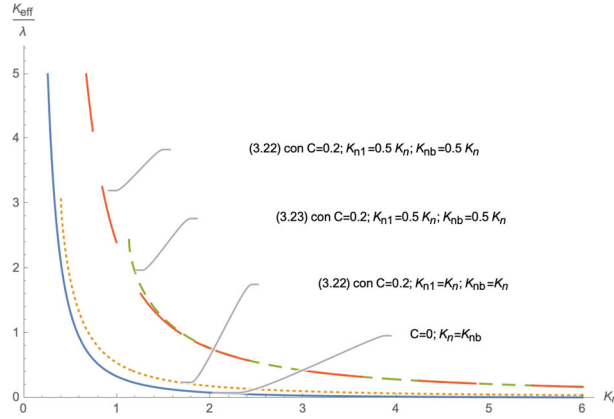


FIG. 3. Sketch of K_{eff} (3.22) and its approximation (3.23) in terms of the phonon Knudsen number $K_n = \ell_{0w}/R$ for different choice of the parameters: a) $C = 0$ and $K_n = K_{nb}$; b) expression (3.22) with $C = 0.2$ and $K_n = K_{nb} = K_{n1}$ or $K_{n1} = 0.5K_n$ and $K_{nb} = 0.5K_n$

A comparison between the effective thermal conductivity (3.22) and its approximation (3.23) is realized in Fig. 3 choosing for the sake of simplicity $C = 0$ and $K_n = K_{nb}$, and $C = 0.2$ with $K_n = K_{nb} = K_{n1}$ or $K_{n1} = 0.5K_n$ and $K_{nb} = 0.5K_n$.

As in (3.18) for $K_{nb} = K_n$, there is the term $\lambda/(3K_n^2)$ plus the term in $\lambda C/K_n$, and a positive nonlinear contribution. In contrast to (3.18), where the nonlinear contribution is of the order of $\frac{\Delta\theta}{L} \frac{K_{n1}}{K_{nb}^2}$ in (3.23) is of the order of $\left(\frac{\Delta\theta}{L}\right)^2 \frac{K_n}{K_{nb}^2} \frac{K_{n2}}{K_{nb}^2}$.

3.3. The m -th q -dependence of $\ell_w(q)$

In the general case, we should consider the full expansion of $\ell_w(q)$ up to the m -th term in (3.9). The solution of the steady equation (3.8) is still (3.13) but with boundary condition (3.9). Following the same procedure, we should find a solution q_w of the equation

$$q_w + C [\ell_{0w} + \ell_{1w}q_w + \ell_{2w}q_w^2 + \ell_{3w}q_w^3 + \dots] \left(\frac{dq}{d\xi}\right)_{wall} = 0, \quad (3.24)$$

which is then substituted in (3.13) and then integrated in order to find K_{eff} .

It is expected that keeping just the highest term in the power series (3.9), we should find that the effective thermal conductivity K_{eff} goes approximatively as

$$K_{eff} = \frac{\lambda}{3K_{nb}^2} + \lambda C \frac{K_n}{K_{nb}^2} \left[1 + C^m \lambda^m \left(\frac{\Delta\theta}{L}\right)^m \left(\frac{K_n}{K_{nb}^2}\right)^{m-1} \frac{K_{nm}}{K_{nb}^2} \right] \quad (3.25)$$

where $K_{nm} = \frac{\ell_{mw}}{R}$.

4. Nonlinear bulk equation

In Sect. 3, we have considered that the mean free path of phonons with respect to phonon–wall collisions appearing in the boundary condition (2.2) depends on q according the expansion (2.4), but we kept the term in ℓ_b appearing in the bulk equation (2.1b) independent of q .

In this section, we assume that ℓ_b may depend on the average value of \mathbf{q} across the layer, q_0 , as stated in (2.6), and ℓ_w , related to phonon–wall collisions, does not depend. The average value q_0 may be found by $q_0 = -K_{eff} \frac{\Delta\theta}{L}$, with K_{eff} the effective thermal conductivity.

However, since ℓ_b appears quadratically in the bulk GK equation, and since the calculations become very complicated and the expressions for K_{eff} very cumbersome, we will limit the contribution of ℓ_b^2 to the first order in q_0 , namely to $\ell_b \approx \ell_{0b} + \ell'_1 q_0$ in (2.7) (that is $m = 1$ in the expansion).

4.1. Bulk nonlinear response

Here, we have instead of (3.8) the bulk equation (2.1b) with $\ell_b = \ell_{0b} + \ell'_1 q_0$

$$\lambda \frac{\Delta\theta}{L} + (\ell_{0b}^2 + 2\ell_{0b}\ell'_1 q_0 + \ell_1'^2 q_0^2) \frac{d^2 q}{dy^2} = 0, \tag{4.1}$$

Here, the mathematical difficulty is higher than that corresponding to nonlinear boundary conditions. As a first approximation, we neglect the term in q_0^2 in ℓ_b^2 such that

$$\lambda \frac{\Delta\theta}{L} + (\ell_{0b}^2 + 2\ell_{0b}\ell'_1 q_0) \frac{d^2 q}{dy^2} = 0, \tag{4.2}$$

The solution is

$$q(y) = -\lambda \frac{\Delta\theta}{L} \frac{y^2}{2\ell_{0b}(\ell_{0b} + 2\ell'_1 q_0)} + c'_2 y + c'_1 \tag{4.3}$$

where we take $c'_2 = 0$ for symmetry of $q(y)$ with respect to $y = 0$. We introduce (4.3) in the boundary condition (2.2) with ℓ_w independent of q . In this way, we will be able to compare the contribution of the bulk with the contribution of the boundary. One will have

$$q(y) = \lambda \frac{\Delta\theta}{L} \frac{1}{2\ell_{0b}(\ell_{0b} + 2\ell'_1 q_0)} (2C\ell_w R + (R^2 - y^2)). \tag{4.4}$$

The average heat flux q_0 may be found as

$$q_0 = \frac{\int_{-R}^R q(y) dy}{2R} = \lambda \frac{\Delta\theta}{L} \frac{R(3C\ell_w + R)}{3\ell_{0b}(\ell_{0b} + 2\ell'_1 q_0)}. \tag{4.5}$$

The above equation leads to the following value of the average heat flux q_0 :

$$q_0 = \frac{-3\ell_{0b}^2 \pm \sqrt{9\ell_{0b}^4 + 24\lambda \frac{\Delta\theta}{L} \ell_{0b}\ell'_1 R(3C\ell_w + R)}}{12\ell_{0b}\ell'_1} \tag{4.6}$$

and hence to the following expression for the effective thermal conductivity

$$K_{eff} = \frac{q_0}{\Delta\theta/L} = \frac{-3K_{nb}^2 \pm \sqrt{9K_{nb}^4 + 24\lambda \frac{\Delta\theta}{L} K_{nb}K'_{n1}(3CK_n + 1)}}{12K_{nb}K'_{n1}\Delta\theta/L} \tag{4.7}$$

where $K_{nb} = \ell_{0b}/R$, $K_n = \ell_w/R$ and $K'_{n1} = \ell'_1/R$.

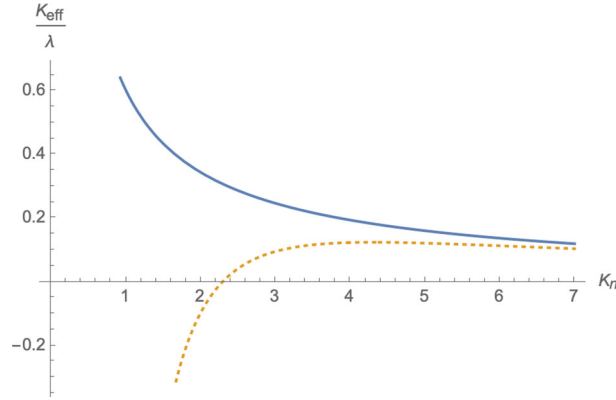


FIG. 4. Sketch of K_{eff} (4.7) (blue line) and (4.9) (dotted yellow line) vs the phonon Knudsen number $K_n = \ell_w/R$ for constant $\Delta\theta/L$ and λ (for the sake of simplicity we have chosen $\Delta\theta/L = 1$ and $\lambda = 1$) and for some values of the parameters: $C = 1$, $K_{nb} = K_n$ and $K'_{n1} = K_n$

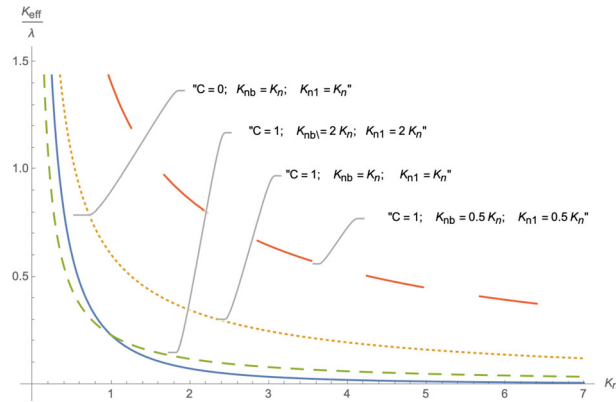


FIG. 5. Sketch of K_{eff} (4.7) vs the phonon Knudsen number $K_n = \ell_w/R$ for constant $\Delta\theta/L$ and λ (for the sake of simplicity we have chosen $\Delta\theta/L = 1$ and $\lambda = 1$) and for some values of the parameters

Expression (4.7) can be also written

$$K_{eff} = \frac{1}{4(\Delta\theta/L)(K'_{n1}/K_{nb})} \left(-1 \pm \sqrt{1 + \frac{8}{3}\lambda \frac{\Delta\theta}{L} \frac{K'_{n1}}{K_{nb}^3} (3CK_n + 1)} \right)$$

in such a way that the argument of the root square may be approximated according to the formula $\sqrt{1+x} \approx 1 + \frac{x}{2} - \frac{x^2}{8}$ with $x = \frac{8}{3}\lambda \frac{\Delta\theta}{L} \frac{K'_{n1}}{K_{nb}^3} (3CK_n + 1)$, which leads to

$$K_{eff} = \frac{1}{4(\Delta\theta/L)(K'_{n1}/K_{nb})} \left(-1 \pm \left(1 + \frac{4}{3}\lambda \frac{\Delta\theta}{L} \frac{K'_{n1}}{K_{nb}^3} (3CK_n + 1) - \frac{8}{9}\lambda^2 \left(\frac{\Delta\theta}{L} \right)^2 \frac{K'^2_{n1}}{K_{nb}^6} (3CK_n + 1)^4 \right) \right). \tag{4.8}$$

The positive sign in the above K_{eff} is

$$K_{eff} = \frac{1}{3}\lambda \frac{(3CK_n + 1)}{K_{nb}^2} - \frac{2}{9}\lambda^2 \left(\frac{\Delta\theta}{L}\right) \frac{K'_{n1}}{K_{nb}^5} (3CK_n + 1)^4. \tag{4.9}$$

In Fig. 4, we plot the positive thermal conductivity (4.7) (the blue line) and the approximated one (4.9) (dotted yellow line) for growing phonon Knudsen number $K_n = \ell_w/R$. For this comparison, we have chosen $\Delta\theta/L = 1$, $\lambda = 1$ and the parameters $C = 1$, $K_{nb} = K_n$ and $K'_{n1} = K_n$ for $K_{nb} = 0.5K_n$.

In Fig. 5 instead, thermal conductivity (4.7) is plotted for different choices of the parameters in order to understand how K_{eff} changes by them.

4.2. Bulk and boundary nonlinear response

In this subsection, we consider again the mathematical model dealt with in the previous subsection, in particular (4.2) with the boundary condition (3.10) instead of (2.2).

The solution is still given by (4.3) with $c'_2 = 0$ because of the symmetry of $q(y)$ with respect to $y = 0$. After introducing (4.3) in the boundary conditions (3.10), we find

$$q(y) = \lambda \frac{\Delta\theta}{L} \left(\frac{R^2 - y^2}{2\ell_{0b}^2 + 4\ell_{0b}\ell'_1 q_0} + \frac{CR\ell_{0w}}{-C\lambda R\Delta\theta/L\ell_{1w} + 2\ell'_1\ell_{0b}q_0 + \ell_{0b}^2} \right) \tag{4.10}$$

The average heat flux q_0 may be found as

$$q_0 = \frac{\int_{-R}^R q(y) dy}{2R} = \frac{1}{3}\lambda R \frac{\Delta\theta}{L} \left(\frac{3C\ell_{0w}}{-C\lambda R\Delta\theta/L\ell_{1w} + 2\ell'_1\ell_{0b}q_0 + \ell_{0b}^2} + \frac{R}{2\ell'_1\ell_{0b}q_0 + \ell_{0b}^2} \right). \tag{4.11}$$

By using $q_0 = K_{eff} \frac{\Delta\theta}{L}$, the above expression becomes

$$K_{eff} = \frac{1}{3}\lambda \frac{1}{K_{nb}^2} \left(\frac{3CK_n}{1 + 2\frac{K'_{n1}}{K_{nb}} K_{eff} \frac{\Delta\theta}{L} - C\lambda \frac{\Delta\theta}{L} \frac{K_{n1}}{K_{nb}^2}} + \frac{1}{1 + 2\frac{K'_{n1}}{K_{nb}} K_{eff} \frac{\Delta\theta}{L}} \right) \tag{4.12}$$

where we have used $K_n = \ell_{0w}/R$, $K_{nb} = \ell_{0b}/R$, $K_{n1} = \ell_{1w}/R$ and $K'_{n1} = \ell'_1/R$. In (4.12), we use the following approximations: $\frac{1}{1+x} = 1 - x + x^2 - x^3 + \dots$ with $x = 2\frac{K'_{n1}}{K_{nb}} K_{eff} \frac{\Delta\theta}{L} - C\lambda \frac{\Delta\theta}{L} \frac{K_{n1}}{K_{nb}^2}$ in the first term and $x = 2\frac{K'_{n1}}{K_{nb}} K_{eff} \frac{\Delta\theta}{L}$ in the second term of the right-hand side. Taking the first two terms of the series, namely $\frac{1}{1+x} \approx 1 - x$, we find

$$K_{eff} = \frac{1}{3}\lambda \frac{1}{K_{nb}^2} \left[3CK_n \left(1 - 2\frac{K'_{n1}}{K_{nb}} K_{eff} \frac{\Delta\theta}{L} + C\lambda \frac{\Delta\theta}{L} \frac{K_{n1}}{K_{nb}^2} \right) + 1 - 2\frac{K'_{n1}}{K_{nb}} K_{eff} \frac{\Delta\theta}{L} \right] \tag{4.13}$$

which leads to

$$K_{eff} = \frac{1}{3}\lambda \frac{1}{K_{nb}^2} \left[(1 + 3CK_n) - 2\frac{K'_{n1}}{K_{nb}} K_{eff} \frac{\Delta\theta}{L} (1 + 3CK_n) + 3C^2 K_n \lambda \frac{\Delta\theta}{L} \frac{K_{n1}}{K_{nb}^2} \right] \tag{4.14}$$

and hence to

$$K_{eff} = \frac{\frac{1}{3}\lambda \frac{1}{K_{nb}^2} \left[(1 + 3CK_n) + 3C^2 K_n \lambda \frac{\Delta\theta}{L} \frac{K_{n1}}{K_{nb}^2} \right]}{1 + \frac{2}{3}\lambda \frac{1}{K_{nb}^2} \frac{K'_{n1}}{K_{nb}} \frac{\Delta\theta}{L} (1 + 3CK_n)} \tag{4.15}$$

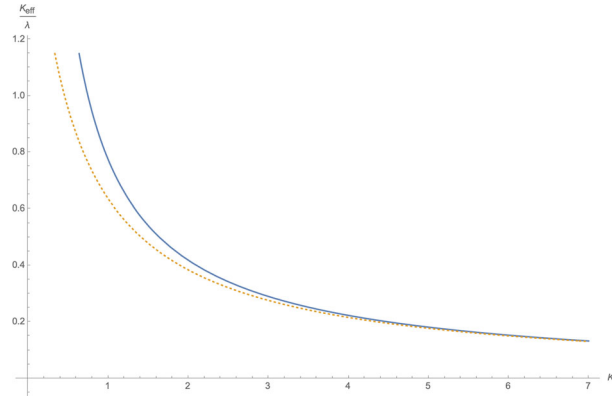


FIG. 6. Sketch of K_{eff}/λ implicitly given by the expression (4.12) (blue line) and the approximated expression (4.15) (dotted yellow line) versus the Knudsen number K_n for constant $\Delta\theta/L$ and for $K_{nb} = K_n$, $K_{n1} = K_n$ and $K'_{n1} = K_n$

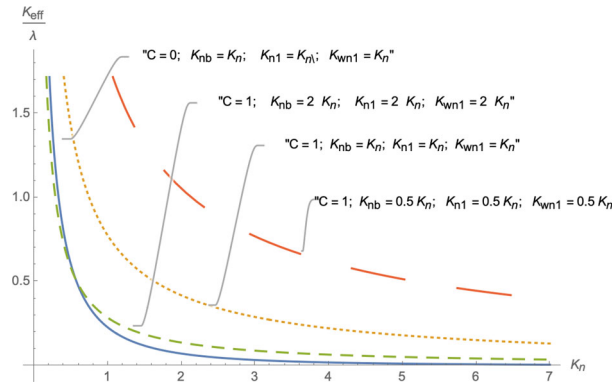


FIG. 7. Sketch of K_{eff}/λ from (4.12) vs the phonon Knudsen number $K_n = \ell_{0w}/R$ for constant $\Delta\theta/L$ (for the sake of simplicity we have chosen $\Delta\theta/L = 1$) and for some values of the parameters C , and the other Knudsen numbers

In Fig. 6, we have compared the ratio K_{eff}/λ implicitly given by the expression (4.12) and the approximated expression (4.15) versus the Knudsen number K_n for $K_{nb} = K_n$, $K_{n1} = K_n$ and $K'_{n1} = K_n$. Expression (4.15) approximates quite well the whole expression (4.12) for high value of the Knudsen number K_n and for the chosen condition on the Knudsen numbers.

In Fig. 7, the thermal conductivity K_{eff} given by (4.12) is shown for some values of the coefficients.

5. Conclusions

In this paper, we have considered nonlinear contributions to the Guyer–Krumhansl equation for the heat flux. The nonlinear effects we have studied arise from a heat flux dependence of the phonon–phonon collisions mean free path ℓ_b (appearing in the GK bulk equation (2.1b)) and of the phonon–wall collisions mean free path ℓ_w (appearing in the slip boundary conditions (2.2)).

In Sect. 2, we have considered the mathematical model given by the Guyer–Krumhansl equation combined with the balance equation of the energy and the boundary condition (2.2). We have assumed that the phonon–wall collisions mean free path ℓ_w may depend on the wall-normal component of the heat flux

\mathbf{q} , namely q_w , and an expansion in power series may be considered for this coefficient. In the case instead of the phonon–phonon collision, mean free path ℓ_b may be composed by two terms, the first being the usual parameter and the second being a perturbation of the first term but depending on the average heat flux q_0 .

In Sect. 3, the linear Guyer–Krumhansl equation combined with the nonlinear contribution in the boundary condition leads to effective thermal conductivity (3.17), which may be approximated into (3.18), and (3.22), which may be approximated into (3.23). In both cases, we have investigated on the contribution of the appearance of heat flux dependence on the effective thermal conductivity with respect to the classical result (2.3). An attempt to grasp the general feature of the thermal conductivity is reported in (3.25), where K_{eff} is found for $\ell_w(q_n) \sim q_n^m$.

In particular, as shown in (3.17) and (3.22), the heat flux is still composed by two main ingredients, the Poiseuille flow and a slip boundary contribution, which are different from the usual one because of the nonlinear contribution. If the coefficient ℓ_{1w} in (3.10) is positive, meaning that the mean free path increases with the heat flux (i.e., the number of phonon–wall collisions per unit length along the nanowire is reduced), expressions (3.17) and (3.18) describe the increase in the effective thermal conductivity K_{eff} along the layer. These results cannot be extrapolated for R too high—in which case K_{eff} should become negative. Indeed, for R sufficiently high, the full equation (2.1b) instead of the simplified form (3.8) must be used.

In Sect. 4, we have instead considered a nonlinear Guyer–Krumhansl equation in the bulk combined with a linear boundary condition in subsection 4.1 (ℓ_w constant), for which we have found the steady-state solution $q(y)$ (4.3) with $c'_2 = 0$, and a nonlinear boundary condition in subsection 4.2 (given by the expression (3.10)). In subsection 4.1, we have found the effective thermal conductivity (4.7) with two branches. Physically, the most realistic would be the positive solution which have been approximated in (4.9). The positive solution and its approximated expression are compared in Fig. 4. In Fig. 5 instead, we have plotted (4.7) for some choices of the parameters. Subsection 4.2 is instead devoted to the combined situation, namely nonlinearity both in the GK equation and in the boundary condition. The results are interesting even though the calculation are quite cumbersome. We have found expression (4.12) with K_{eff} inside. Some efforts have been required for making K_{eff} explicit, as shown in (4.15). The two expressions (4.12) and (4.15) are compared in Fig. 6. In Fig. 7 instead, expression (4.12) is plotted for different values of the parameters.

The expressions for the effective thermal conductivity may be expanded in powers of the heat gradient, which, in turn, also depend on powers of the Knudsen numbers. This is in contrast with the heuristic power-law model for non-Newtonian phonon hydrodynamics proposed in [30], in analogy with the well-known power-law rheological model for non-Newtonian viscous fluids, where the effective thermal conductivity depends on the heat gradient and on the Knudsen numbers in a fractional exponent. That model leads to simpler mathematical expressions than the present model; in it, the mean free paths depend on the gradient of the heat flux rather than on the heat flux itself, as it has been assumed here. In principle, both possibilities should be considered.

Acknowledgements

D.J. acknowledges the financial support from the Università degli studi di Palermo for his visit in July 2024. M.S. acknowledges the financial support from the PRIN project 2022TMW2PY_002 “Transport phonema in low dimensional structures: models, simulations and theoretical aspects”—project code 2022TMW2PY—CUP B53D23009500006. This paper is partially supported by the PNRR project ECS00000022 “SiciliAn MicronanOTech Research And Innovation Center (SAMOTHRACE)” and the project H2020-ECSEL-2017-1-IA-two-stage “first and european sic eightinches pilot line-REACTION”.

Author contributions M.S. and D.J. wrote the main manuscript text. M.S. prepared figures. All authors reviewed the manuscript.

Funding Open access funding provided by Università degli Studi di Palermo within the CRUI-CARE Agreement.

Data availability No datasets were generated or analyzed during the current study.

Declarations

Conflict of interest The authors declare no conflict of interest.

Open Access. This article is licensed under a Creative Commons Attribution 4.0 International License, which permits use, sharing, adaptation, distribution and reproduction in any medium or format, as long as you give appropriate credit to the original author(s) and the source, provide a link to the Creative Commons licence, and indicate if changes were made. The images or other third party material in this article are included in the article's Creative Commons licence, unless indicated otherwise in a credit line to the material. If material is not included in the article's Creative Commons licence and your intended use is not permitted by statutory regulation or exceeds the permitted use, you will need to obtain permission directly from the copyright holder. To view a copy of this licence, visit <http://creativecommons.org/licenses/by/4.0/>.

Publisher's Note Springer Nature remains neutral with regard to jurisdictional claims in published maps and institutional affiliations.

References

- [1] Cimmelli, V.A.: Different thermodynamic theories and different heat conduction laws. *J. Non Equilib. Thermodyn.* **34**, 299–333 (2009)
- [2] Straughan, B.: *Heat waves* 177. Springer, Berlin (2011)
- [3] Joseph, D.D., Preziosi, L.: *Heat waves*. *Rev. Mod. Phys.* **61**(1), 41 (1989)
- [4] Tzou, D.Y.: *Macro-to microscale heat transfer: the lagging behavior*. Wiley, Hoboken (2014)
- [5] Sellitto, A., Cimmelli, V.A., Jou, D.: *Mesoscopic theories of heat transport in nanosystems* 6. Springer, Berlin (2016)
- [6] Mongiovì, M.S., Jou, D., Sciacca, M.: Non-equilibrium thermodynamics, heat transport and thermal waves in laminar and turbulent superfluid helium. *Phys. Rep.* **726**, 1–71 (2018)
- [7] Lebon, G., Jou, D., Casas-Vàzquez, J.: *Understanding non-equilibrium thermodynamics*. Springer-Verlag, Berlin (2008)
- [8] Kovács, R., Ván, P.: Generalized heat conduction in heat pulse experiments. *Int. J. Heat Mass Transf.* **83**, 613–620 (2015)
- [9] Galenko, P., Jou, D.: Rapid solidification as non-ergodic phenomenon. *Phys. Rep.* **818**, 1–70 (2019)
- [10] Chen, G.: Non-Fourier phonon heat conduction at the microscale and nanoscale. *Nat. Rev. Phys.* **3**(8), 555–569 (2021)
- [11] Benenti, G., Donadio, D., Lepri, S., Livi, R.: Non-fourier heat transport in nanosystems. *La Rivista del Nuovo Cimento* **46**(3), 105–161 (2023)
- [12] Guyer, R.A., Krumhansl, J.: Solution of the linearized phonon Boltzmann equation. *Phys. Rev.* **148**, 766–778 (1966)
- [13] Guyer, R.A., Krumhansl, J.: Thermal conductivity, second sound and phonon hydrodynamic phenomena in nonmetallic crystals. *Phys. Rev.* **148**, 778–788 (1966)
- [14] Ván, P., Berezovski, A., Fülöp, T., Gróf, G., Kovács, R., Lovas, Á., Verhás, J.: Guyer-krumhansl-type heat conduction at room temperature. *Europhys. Lett.* **118**(5), 50005 (2017)
- [15] Alvarez, F.X., Jou, D., Sellitto, A.: Phonon hydrodynamics and phonon-boundary scattering in nanosystems. *J. Appl. Phys.* **105**, 014317 (2009)
- [16] Larecki, W., Banach, Z.: Influence of nonlinearity of the phonon dispersion relation on wave velocities in the four-moment maximum entropy phonon hydrodynamics. *Physica D* **266**, 65–79 (2014)
- [17] Guo, Y., Wang, M.: Phonon hydrodynamics and its applications in nanoscale heat transport. *Phys. Rep.* **595**, 1–44 (2015)
- [18] Lebon, G.: Heat conduction at micro and nanoscales: a review through the prism of extended irreversible thermodynamics. *J. Non-Equilib. Thermodyn.* **39**, 35–59 (2014)
- [19] Sellitto, A., Carlomagno, I., Jou, D.: Two-dimensional phonon hydrodynamics in narrow strips. *Proc. R. Soc. A: Math., Phys. Eng. Sci.* **471**(2182), 20150376 (2015)
- [20] Ghosh, K., Kusiak, A., Battaglia, J.-L.: Phonon hydrodynamics in crystalline materials. *J. Phys.: Condens. Matter* **34**(32), 323001 (2022)

- [21] Banach, Z., Larecki, W.: Nine-moment phonon hydrodynamics based on the modified grad-type approach: formulation. *J. Phys. A: Math. Gen.* **37**(41), 9805 (2004)
- [22] Cepellotti, A., Fugallo, G., Paulatto, L., Lazzeri, M., Mauri, F., Marzari, N.: Phonon hydrodynamics in two-dimensional materials. *Nat. Commun.* **6**(1), 6400 (2015)
- [23] Geim, A.K., Novoselov, K.S.: The rise of graphene. *Nat. Mater.* **6**(3), 183–191 (2007)
- [24] Balandin, A.A., Ghosh, S., Bao, W., Calizo, I., Teweldebrhan, D., Miao, F., Lau, C.N.: Superior thermal conductivity of single-layer graphene. *Nano Lett.* **8**(3), 902–907 (2008)
- [25] Balandin, A.A.: Thermal properties of graphene and nanostructured carbon materials. *Nat. Mater.* **10**(8), 569–581 (2011)
- [26] Li, X., Lee, S.: Role of hydrodynamic viscosity on phonon transport in suspended graphene. *Phys. Rev. B* **97**(9), 094309 (2018)
- [27] Asheghi, M., Leung, Y., Wong, S., Goodson, K.: Phonon-boundary scattering in thin silicon layers. *Appl. Phys. Lett.* **71**(13), 1798–1800 (1997)
- [28] Bernini, U., Lettieri, S., Maddalena, P., Vitiello, R., Di Francia, G.: Evaluation of the thermal conductivity of porous silicon layers by an optical pump-probe method. *J. Phys.: Condens. Matter* **13**(5), 1141 (2001)
- [29] Usenko, A.Y., Carr, W.N., Chen, B.: Transfer of single-crystalline silicon nanolayer onto an alien substrate. *Nanotechnology* **5118**, 474–481 (2003)
- [30] Sciacca, M., Jou, D.: A power-law model for nonlinear phonon hydrodynamics. *Z. Angew. Math. Phys.* **75**(2), 70 (2024)
- [31] Dong, R.-Y., Dong, Y., Sellitto, A.: An analogy analysis between one-dimensional non-fourier heat conduction and non-newtonian flow in nanosystems. *Int. J. Heat Mass Transf.* **164**, 120519 (2021)
- [32] Jou, D., Casas-Vázquez, J., Lebon, G.: *Extended Irreversible Thermodynamics*. Berlin: Springer-Verlag, fourth ed., (2010)
- [33] Müller, I., Ruggeri, T.: *Rational extended thermodynamics*. Springer-Verlag, New York (1998)
- [34] Berezovski, A., Ván, P.: *Internal variables in thermoelasticity*. Springer, Berlin (2017)

Michele Sciacca
Dipartimento di Ingegneria
Università di Palermo
Viale delle Scienze
90128 Palermo
Italy

Michele Sciacca
Istituto Nazionale di Alta Matematica
Roma 00185
Italy
e-mail: michele.sciacca@unipa.it

David Jou
Departament de Física
Universitat Autònoma de Barcelona
Bellaterra, Catalonia
Spain
e-mail: david.jou@uab.cat

David Jou
Institut d'Estudis Catalans
Carme 47
08193 Barcelona, Catalonia
Spain

(Received: January 6, 2025; revised: January 6, 2025; accepted: March 24, 2025)